Detonation Simulation with the AMROC Framework

Ralf Deiterding
Center for Adanced Computing Research

California Institute of Technology
1200 East California Blvd., Mail-Code 158-79
Pasadena, CA 91125
ralf@cacr.caltech.edu

Governing Equations

Multi-component reactive Euler equations for thermally perfect gases with general equation of state

$$p(\rho,T)=\sum_{i=1}^{K}p_i=\sum_{i=1}^{K}\rho_i\frac{\mathcal{R}}{W_i}T\,.$$

Caloric equation:

$$h(\rho,T)=\sum_{i=1}^{K}Y_ih_i(T)\quad\text{with}\quad h_i(T)=h_i^0+\int_0^T c_{pi}(s)ds$$

Evaluation of $p(\rho,T)$ requires computation of $T=T(\rho,e)$ from implicit equation

$$\sum_{i=1}^{K}\rho_i\,h_i(T)-\mathcal{R}T\sum_{i=1}^{K}\frac{\rho_i}{W_i}-\rho e=0\,.$$

Non-equilibrium Arrhenius kinetics for $H_2:O_2$ combustion:

- 34 elementary reactions.
- 9 species: H, O, OH, H_2, O_2, H_2O, HO_2, H_2O_2,Ar.

Numerical Methods

Numerical source term incorporation and extension to multiple dimensions with method of fractional steps. $\longrightarrow$ Numerical decoupling of hydrodynamic and chemical time steps.

Time-explicit finite volume shock-capturing method:

- Upwinding with Roe-linearization for thermally perfect gases.
- Avoids unphysical densities and energies by switching to HLL.
- Preserves mass fraction positivity.
- Entropy and carbuncle fix.
- 2nd-order MUSCL reconstruction.

Source term integration:

- Standard solver for stiff ODE's, e.g. semi-implicit Rosenbrock-Wanner method.
- Automatic stepsize adjustment to allow for an efficient treatment of chemical time scales smaller than the global time-step.

Locally high resolution, which is essential for the accurate computation of detonation waves, is achieved by blockstructured adaptive mesh refinement (AMR).

- Discretization necessary only for single rectangular grid.
- Spatial *and* temporal refinement, no global time step restriction.
- Blockstructured data gurantees high computational performance.

Cellular Structure Simulation in 2D

Experiments have shown that self-sustaining detonation waves are locally multi-dimensional and nonsteady. Triple-points form, which enhance the local chemical reaction significantly.

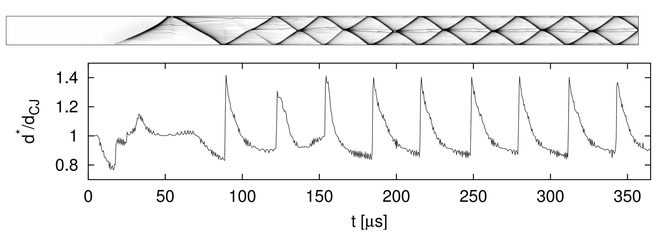

Low-pressure $H_2:O_2$ detonations with high Ar diluent show a very regular triple point pattern. Lower plot: detonation velocity along lower boundary.

- ≈ 45 cells within induction length.
- Adaption criteria:
  1. Scaled gradients $|Q^n_{i+1}-Q^n_i|$ of p and ρ
  2. Estimation of error in Y_i by Richardson extrapolation

$$\begin{matrix}Q^n & \overset{\Delta t,\Delta x}{\Longrightarrow} & \tilde{Q}\\ Q^{n-1} & \overset{2\Delta t,2\Delta x}{\Longrightarrow} & \hat{Q}\end{matrix}\qquad \tau=\frac{|\tilde{Q}-\hat{Q}|}{2^{d+1}-2}$$

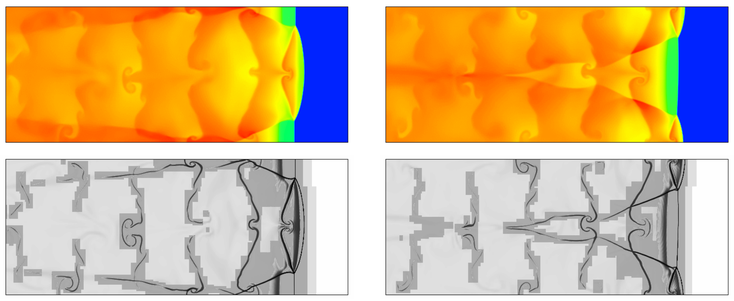

Color plots of the temperature and schlieren plots of the density on refinement regions in the first (left) and second half (right) of a detonation cell.

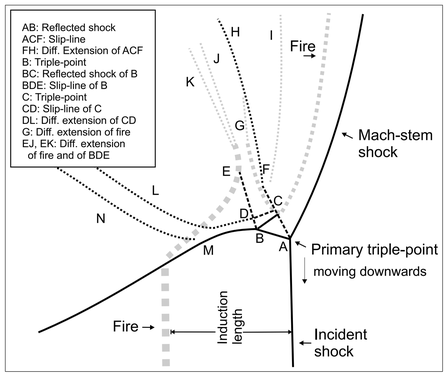

Schematic diagram of the flow around a triple-point.

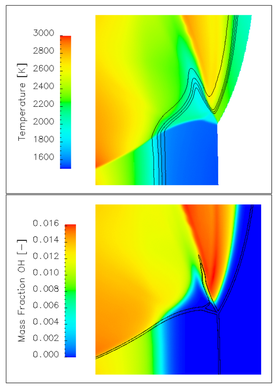

Flow around a triple-point. Additional isolines show the induction length.

Cellular Structure in 3D

- Quasi-stationary computation. Symmetric in x_2-direction.
- ≈ 16.8 cells within induction length.
- Adaptive computation uses 1.0M-1.5M cells. (Nonadaptive 8.8M).

Task	%
Hydrodynamics	36.7
Kinetics	20.3
Boundaries	38.4
Recomposition	1.9
Misc.	2.7
CPU [h]	3800

Breakdown of computating time.

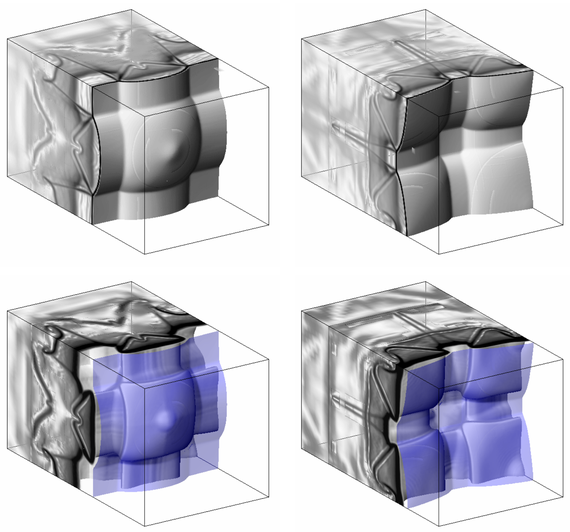

Right: Schlieren plots of density (upper row) and mass fraction of OH (lower row) in the first (left) and second (right) half of detonation cell. The blue isosurface visualizes the induction length.

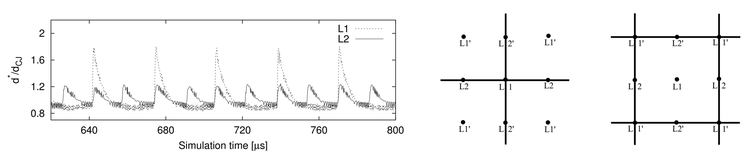

Left: Temporal development of the detonation velocity along L1 and L2. Right: Point-wise reinitiation along L1 (left) and L1' (right). The time between both situations is a half oscillation period.

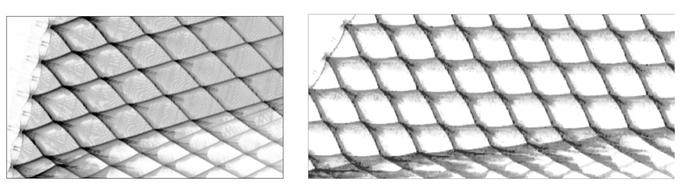

Simulated triple point tracks for 2D detonations reflected under inflow angles $\Theta=15^o$ (left) and $\Theta=30^o$ (right).

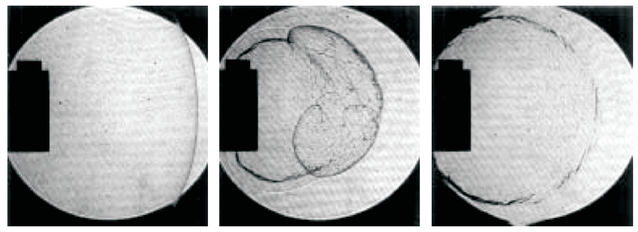

Left: successful transmission. Middle: critical. Right: subcritical, detonation failure.

Detonation Diffraction

The simulation reproduces exactly the experimentally measured *critical tube diameter* of 10 detonation cells width.

- ≈ 25 cells within induction length.
- Adaptive computation uses around 3 M cells. (Nonadaptive 150 M)
- 4600h CPU time on 48 Athlon-1.4 GHz nodes.

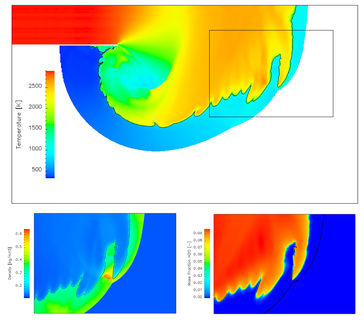

Detonation failure for a tube width of 8 detonation cells.

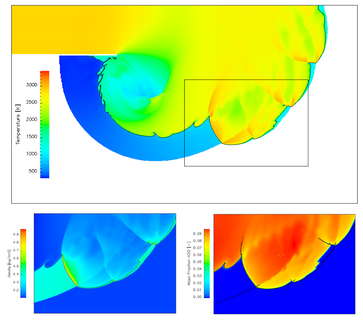

Successful transmission for a tube width of 10 detonation cells.

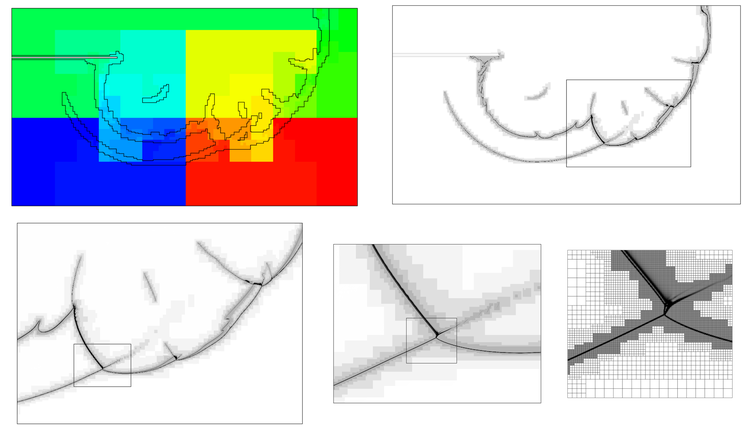

Top, left: Final distribution to 48 nodes. The domains are indicated by color. Other graphics: Density distribution on four refinement levels. Multiple zooms are necessary to display the finite volume cells (lower right graphic).

Mach Reflection of a Detonation

For larger inflow angles a detonation wave is reflected in form of a Mach reflection. The higher overdrive factor in the Mach stem region suppresses the triple points (see left triple point track).

- ≈ 20 cells within induction length.
- Adaptive computation uses around 1.2 M cells. (Nonadaptive 59 M)
- 1200h CPU time on 16 Pentium-III-850 MHz nodes.

Schlieren plot of the density $t=48\,\mu$s after hitting the wedge. Left: $\Theta=15^o$, right: $\Theta=30^o$.